Published in final edited form as:
Cryogenics (Guildf). 2017 December ; Volume 88: 36–43. doi:10.1016/j.cryogenics.2017.10.010.

Cryogenic thermal conductivity measurements on candidate materials for space missions

James Tuttle[a], **Edgar Canavan**, **Amir Jahromi**
NASA Goddard Space Flight Center, Code 552, Greenbelt, MD 20771, USA

Abstract

Spacecraft and instruments on space missions are built using a wide variety of carefully-chosen materials. It is common for NASA engineers to propose new candidate materials which have not been totally characterized at cryogenic temperatures. In many cases a material's cryogenic thermal conductivity must be known before selecting it for a specific space-flight application. We developed a test facility in 2004 at NASA's Goddard Space Flight Center to measure the longitudinal thermal conductivity of materials at temperatures between 4 and 300 Kelvin, and we have characterized many candidate materials since then. The measurement technique is not extremely complex, but proper care to details of the setup, data acquisition and data reduction is necessary for high precision and accuracy. We describe the thermal conductivity measurement process and present results for ten engineered materials, including alloys, polymers, composites, and a ceramic.

Keywords

Cryogenic; thermal conductivity

INTRODUCTION

Many of NASA's scientific space missions include instruments which operate at cryogenic temperatures. For these missions, both the spacecraft and the instruments are built using materials specifically chosen for optimum performance. They must all survive the launch and the space environment, and some have additional requirements on their thermal conductivity. Structural elements must be stiff and strong, but they must not conduct excessive heat from the warm to the cold parts of the spacecraft. Electrical cables must provide wires with appropriate electrical resistance, and they must include sufficient insulation and shielding. However, when these cables run from a room-temperature electronics box to a cryogenic instrument, they must not conduct more heat than the cooling system can handle. Thermal radiator backing plates must be structurally sound and have very high thermal conductivity. In general, all objects on a NASA mission must be as light as possible. Projects often identify engineered materials, such as alloys, polymers and composites, as candidates to meet these requirements, based on known room temperature

[a]Corresponding author: james.g.tuttle@nasa.gov.

properties. As a result, NASA often finds itself in need of thermal conductivity data on materials at cryogenic temperatures.

In support of the James Webb Space Telescope (JWST), we developed a test facility in 2004 at NASA's Goddard Space Flight Center to measure the thermal conductivity of materials between 4 and 300 Kelvin. These measurements are longitudinal, meaning that they determine the conductivity of heat along a significant length of material rather than normal to the plane of a thin material sheet. Nearly all of the thermal conductivity measurements that JWST needed were longitudinal.

The thermal conductivity, κ, is generally a function of temperature, and its MKS units are W/m/K. The general approach to measuring κ is to cause heat to flow through a constant-cross-section sample and determine the temperature gradient. To get high-precision thermal conductivity data, we chose to perform absolute measurements. This is in contrast to comparative methods, in which calibrated thermal conductance standards are installed in the test set-up along with the sample to be characterized. In one such comparative approach, the sample is located between two standards, to which it is thermally linked in series[1]. Heat flows through this assembly, and the temperature drop across the sample is compared to the drops across the standards. The ratio of these temperature drops is inversely proportional to the ratio of thermal conductances, so the sample's thermal conductivity can be determined.

For high-precision measurements, this comparative approach poses some problems. The standards must have been characterized to at least as high precision as that desired for the sample measurement. In addition, they must have conductances reasonably close to that of the sample (which is initially unknown). A mismatch in these conductances increases the uncertainty in backing out the sample conductance, and at higher temperatures it stymies efforts to limit the heat loss via thermal radiation. Nearly all candidate materials for use as a standard have batch-to-batch thermal conductivity variations of at least a few percent in the cryogenic temperature range. That suggests that in most cases a custom absolute thermal conductance measurement must be done ahead of time on each standard, with significant cost and logistical impact. For high-precision data it makes sense to perform an absolute measurement on the sample itself.

We chose an approach which has been described elsewhere[2]. Our specific implementation of this approach has also been described before[3,4], but we have improved details of the setup, data acquisition and data reduction over time. Since developing our test facility, we have characterized many materials for JWST and other programs. Our goal here is to both share the thermal conductivity data and to provide guidance to other researchers who may wish to perform similar measurements themselves.

MEASUREMENT CHALLENGES

Most absolute thermal conductivity measurements involve establishing steady "thermal balance" states in a sample having uniform cross sectional area along its length. In each such balance, heat is generated in a resistive heater mounted on the "floating" end of the sample. The applied power is the product of the electrical current flowing through the heater and the

voltage drop across it, both of which can be measured to very high precision by standard multi-meters. The sample's other end is thermally attached to a heat sink referred to as the "base," at a slightly lower temperature. An idealistic assumption is that the sample exchanges no heat with its surroundings, and only conducts heat from the heater to the base. If this were the case, in this steady state, with a small temperature drop across the sample, it would be true to a very close approximation that

$$\kappa(\bar{T}) = \frac{L\dot{Q}}{A\,\Delta T}. \quad (1)$$

Here $\dot{Q}$ is the conducted heat, $\bar{T}$ is the average of the temperatures at the two sample ends, ΔT is the difference between these temperatures, L is the sample length, and A is the sample's cross-sectional area. Assuming that a researcher can install and operate compact heaters and thermometers, it might seem that an absolute thermal conductivity measurement is a straightforward endeavor. One simply measures the sample's end temperatures and the corresponding heater power, and equation (1) gives the thermal conductivity at the average temperature. Figure 1 is a schematic representation of the basic set-up for this approach. Note that an isothermal can, attached to the base, surrounds the sample to eliminate thermal radiation heat exchange with nearby surfaces at much higher or lower temperatures.

Unfortunately, there are a number of complications involved in this approach. Some of them will seem obvious and easily-solvable to experienced cryogenic researchers. Others are only important for high-precision measurements. However, a perusal of the literature has shown that some researchers are ignoring each of these issues in their attempts to measure thermal conductivity. We have found that only a modest amount of extra effort is needed to address these issues, so we will discuss all of them here.

First, the heat conducted through the sample, $\dot{Q}$, is not equal to the measured heater power, $\dot{Q}_H$. Some heat is conducted away from the sample's floating end via the thermometer's electrical leads. The heater's leads present a more complicated issue, as they carry significantly more current than those of the thermometer. Ohmic heat is generated in these leads, and in some cases a fraction of this heat is conducted into the heater itself. Thus, the net heat conducted away from the heater via its leads may end up being either positive or negative.

At higher temperatures, a significant amount of heat passes directly from the heater and sample to the base and its can via thermal radiation. It may seem that this issue can be mitigated by always using small ΔT values across the sample, but this is not true. The radiative heat exchange between two objects at different temperatures, T_{Hot} and T_{Cold}, is proportional to $T_{Hot}^4 - T_{Cold}^4$. However, for small values of $\Delta T = T_{Hot} - T_{Cold}$, it is easy to show that

$$T_{Hot}^4 - T_{Cold}^4 \sim 4\bar{T}^3 \Delta T, \quad (2)$$

where $\bar{T}$ is the average of the two temperatures. This approximation becomes more accurate as ΔT decreases relative to $\bar{T}$. Thus, for small ΔT values, the heat radiated from any location

on the sample to its surroundings at the base temperature is proportional to ΔT, as is the heat conducted through the sample. For any given average temperature, this radiated heat will give the same relative error in the thermal conductivity measurement, independent of ΔT.

The most convenient locations for thermometers in such an experiment are generally on the base and on the sample's floating end heater assembly, as shown in Figure 1. However, the indicated total temperature drop is then not equal to the temperature drop across the sample. There are thermal joint resistances associated with the heater's attachment to the floating end and the sample's attachment to the base. Since heat flows through these joints, there is a localized temperature drop across each of them, and the indicated total ΔT includes these temperature drops. In addition, the temperature indicated by a thermometer has an error, δT, at any temperature due to scatter in its temperature vs. resistance calibration curve.

The issues listed here result in uncertainties in the power flowing through the sample and the temperature drop across it, leading to a significant uncertainty in the thermal conductivity. We describe below a configuration which drastically reduces the magnitude of several of these uncertainties and a data acquisition and analysis approach which makes the remaining ones nearly irrelevant.

GENERAL SET-UP

Figure 2 shows our measurement configuration roughly to-scale, with a sample length of about 9 cm. It is installed on the cold plate of a cryostat and surrounded by a nearly-isothermal cold plate shield. The cold plate is cooled to temperatures as low as 3 K by a standard two-stage cryocooler. The sample bottom is clamped to a copper base, which is located above the cold plate on a stainless-steel support tube. A heater and thermometer on the base allow it to be controlled at any chosen temperature between about 4 and 300 K. An aluminum heater assembly clamps to the floating (top) end of the sample. Installed on this assembly are the sample heater and sample thermometer, allowing it to be independently controlled at temperatures above that of the base.

Two thermometers are bonded to metallic "thermal taps" at intermediate locations along the middle region of the sample. We refer to these as "near" and "far" thermometers, indicating their relative distances from the base. To determine the thermal conductivity, we use these tap temperatures and the length between them rather than the base and heater temperatures and the total sample length. This eliminates the effect of joint resistances at the sample ends.

The taps vary in design, depending on characteristics of the sample being tested. For low-thermal-conductivity materials, the taps are often pairs of narrow aluminum strips which straddle the sample as indicated in Figure 2. Tiny screws running through a pair of these strips allow them to clamp onto opposite sides of the sample at the same vertical location. Since the aluminum is much more thermally conductive than such a sample material, we assume that the taps thermally "short" the sample over the small parts of its length which they contact. Thus, the effective thermal length between the taps is taken as the distance between their nearest (facing) horizontal surfaces. For higher-thermal-conductivity materials, the taps are either copper wires or pieces of sheet copper with holes exactly

matching the sample cross section. In this case, each tap is bonded to the sample with a small bead of epoxy, and the thermal length between them is taken as the vertical distance between their centers

A removable cylindrical “guard” surrounds the sample. This guard consists of a stainless-steel tube with copper flanges soldered to its top and bottom ends. The bottom flange, which bolts to the base, is the same height as the clamp holding the sample bottom. Also, the top flange’s bottom is at the same height as the bottom of the sample heater assembly. The top flange extends about a cm above the top of the sample, and a copper cover is bolted to its top. Small, connected horizontal and vertical holes in the base allow the guard’s volume to be evacuated, while baffling any thermal radiation.

A heater wrapped around the top flange and a thermometer on its outside allow it to be independently controlled at temperatures above that of the base. The region inside the guard, surrounding the sample, is loosely filled with a fibrous insulation called Fiberfrax. This material has a very low thermal conductivity, proportional to T^3, which has been independently measured between 80 K and room temperature[2]. A copper can, bolted at its bottom to the base, completely surrounds the guard. A thin multi-layer blanket covers this can, and another disk-shaped blanket is installed inside the base’s stainless-steel support tube. These blankets minimize temperature gradients in the base and its can caused by thermal radiation to the cold cryostat surroundings.

During each measurement balance, the guard’s top flange and the sample’s floating end are always independently controlled at the same temperature. For small ΔT values, this results in sample and guard temperature profiles that match nearly identically. Thus, there is nearly zero thermal radiation between the sample and guard in the radial direction. Any radiation in the axial direction is reduced to nearly zero by the fibrous insulation. A finite-element thermal model, discussed later, supports the fact that the guard and insulation effectively eliminate the loss of heat from the sample by thermal radiation.

THERMOMETERS AND THEIR LEADS

Thermometers used in this apparatus are calibrated SD-package Cernox™ sensors[5]. For these resistive devices, the actual sensing chip is inside a 1 × 2 × 3 mm hermetic box. This compact packaging is essential for installation on the very small surfaces of our sample thermal taps. Unfortunately, these tiny sensors come with two approximately two-cm-long straight copper “terminals” to which the electrical leads must be soldered. It is possible to shorten these terminals by cutting them, but then precautions must be taken not to overheat the sensor during the soldering process. Alternatively, the terminals can be folded back on themselves after soldering to reduce their profile, but care must be taken not to break them or pull them off the sensor package. We hope that in the future LakeShore Cryotronics will provide a standard SD package configuration in which they directly solder isolating leads onto the sensor package, eliminating these copper terminals.

Cryogenic thermometers are read out via four electrical leads. Two leads conduct the excitation current, and two are used to measure the resulting sensor voltage. Since the

current is extremely low, there is essentially no ohmic heating in the leads for any practical wire resistance values. Thus, the leads wires can be selected to have very high electrical and thermal resistance. When purchasing thermometers with leads installed by LakeShore Cryotronics, we opt for their smallest-diameter phosphor-bronze leads. When we choose to install our own leads, we use custom-made 0.06 or 0.13 mm diameter cupro-nickel-clad stainless-steel wire, which is stronger and less thermally conductive than phosphor bronze wire of the same diameter.

Proper installation of an SD-package thermometer involves thermally attaching its electrical leads to the surface on which the thermometer is mounted. We bond thermometers and leads to the taps using varnish, which can later be dissolved with alcohol to allow removal of the thermometers without damaging them. We also varnish the far thermometer's leads to the sample heater assembly, ensuring that all heat flowing through the middle part of the sample originates at the sample heater.

The leads from the near thermometer are thermally attached to the base as they exit it through epoxy-filled holes. All leads from the sample heater assembly similarly exit the guard's top flange. This detail is particularly important. Since the tops of the sample and guard are kept at the same nominal temperature in each balance, we expect to have zero heat conducted through the leads running between them. Thus, the guard serves a second purpose, eliminating heat loss through electrical leads.

One further step is taken to reduce the heat conducted by the thermometer leads. Between any two of their thermal attachment locations within the guard, each thermometer's leads are coiled so that they follow a spiral path. This is accomplished by temporarily tightly-wrapping them around a small-diameter rod before installing the thermometer. This coiling can increase the effective thermal length along the leads by as much as an order of magnitude.

HEATERS AND THEIR LEADS

The sample heater and its current leads are engineered to minimize heat generated in these leads inside the guard. As with the sample thermometer, both ends of these leads are held at the same temperature during balance. However, the heater current is much higher than that used in the thermometers. About half of the ohmic heat generated in these leads is conducted into the heater, but it is not part of the heater power measured as the product of its current and voltage. Rather than try to calculate and correct for this extra heat, we minimize it by keeping the lead resistance more than 100 times lower than the heater resistance. We don't use copper leads heater leads here, as we generally prefer to keep their thermal conduction from being too high. Our sample heater is a small 10 KΩ metal-film resistor epoxied onto the aluminum heater clamp. Its leads currently contain 0.13 mm diameter stainless steel wires, but in the past they have been made from excess LakeShore phosphor bronze thermometer leads. Their round-trip resistance inside the guard is less than ten ohms, so the extra heat from the leads is less than 0.1% of the measured heater power and can be ignored. The electronic controller box powers this heater with up to 50 volts, and the resulting 0.25 Watt heater power is sufficient for all of our thermal balances.

The heaters on the base and the guard's top flange are used for temperature control, but their actual power values are not measured. They are made of 0.13 mm diameter stainless steel wire wound around and epoxied to the respective stages, with resistances of approximately 50 ohms. Their current leads are 0.25 mm diameter copper, and in our system they can provide up to 50 Watts.

INSTRUMENTATION

The thermometers are read using three Cryogenic Control Systems, Inc. Model 32B temperature controllers. Each of these devices can read two thermometers simultaneously and can provide proportional-integral-differential (PID) control of their temperatures via two independent heater circuits. We control the temperatures of the base and the sample and guard floating ends, and we monitor the near, far, and cryostat cold plate thermometers. With acceptable time-averaging, these temperatures can be resolved and held stable to better then 0.1 mK RMS at our lowest temperatures and about 1 mK at room temperature. The sample heater current and voltage are read constantly with two Keithley model 2000 6.5-digit multi-meters.

Each thermometer is read by measuring its resistance, and the temperature is determined using a calibration file provided by LakeShore Cryotronics. This file is loaded into the temperature controller box, which uses a cubic spline interpolation algorithm to convert measured resistances into temperatures. The box then reports temperature values directly to the data acquisition program. For our selected thermometers, a calibration file contains about 80 discreet temperature/resistance pairs between 1.2 and 330 Kelvin. The temperature difference between consecutive calibration points increases with rising temperature. At 4 Kelvin they are about 0.2 K apart, and from 100 to 300 K the spacing is 10 K.

VACUUM ISSUES

For obvious reasons, our measurement must take place in a vacuum environment. Our standard practice, for other types of cryogenic tests, is to pump on our sealed cryostats for at least 15 hours with a turbo-mechanical pump before powering on the cryocoolers. A cold cathode gauge, attached directly to a cryostat's vacuum shell, is used to confirm that the pressure reaches the acceptably low range of about 0.1 mTorr during this time. After the cooldown, our experiments are inside a sub-ten-Kelvin shield attached to the cold plate, and this is surrounded by another shield at about 50 Kelvin. Any small flow of air or water vapor from the outer vacuum shell freezes on these shields before reaching the experiment. Inside the cold plate shield, the partial pressure of all gases other than helium or hydrogen is essentially zero. A charcoal getter installed on the cold plate next to our experiment ensures that even these gases will be adsorbed, and their pressures are trivially low.

We learned recently that under certain circumstances a cold cathode gauge can split water molecules and create a flow of hydrogen gas[6]. This hydrogen does not freeze on the outer shield, and its flow to the getter may eventually result in a non-zero pressure inside the inner shield. To avoid this problem, we only power on the gauge for short periods of time to check the vacuum, leaving it off at all other times.

However, there is an additional concern during our thermal conductivity measurements, for which the critical volume is inside the guard. At room temperature, the FiberFrax insulation is capable of absorbing a significant amount of water from the air. The pump-out path for the guard has a relatively high flow impedance, so it takes a long time to dry out the Fiberfrax. For low cryogenic sample temperatures, this is not a problem, as the water remains frozen on the fibers with essentially zero vapor pressure. However, when measurements are take closer to room temperature, water resumes evaporating from the fibers, and the pressure inside the guard rises. This produces an additional conductive path for the sample heat, and it can lead to a resolvable error in our data. The cold plate shield does not mitigate this problem, aside from very slowly cryopumping the water vapor away.

Thus, it is essential that we dry out the Fiberfrax before cool-down. To facilitate this process, we use the sample heater as an effective pressure gauge. During the cryostat pump-out period, we control the base temperature at 320 K. The guard temperature is not controlled, but the sample's floating end is held at 321 K. After these temperatures have stabilized, we monitor the sample heater's controlling power. Because of the mismatch between sample and guard temperatures, there is a pressure-dependent heat flow from sample to guard. This results in a slow, downward trend in the sample controlling power over time, eventually reaching a constant value after about 48 hours. We interpret this steady power as an indication that the water vapor pressure is no longer significant. Since we generally don't take thermal conductivity data above 295 Kelvin, the water vapor pressure should always be even lower than it was at the end of our bake-out.

DATA ACQUISITION

A computer is interfaced to the temperature controllers and multimeters, and we have written two different LabView software routines for data acquisition. One routine allows manual control of the measurements. It displays continuous graphs of thermometer and sample heater power readings and allows a user to change each control channel's temperature set-points and PID parameters. New measurements are taken 5 to 10 times per second, but each graphed point has been time-averaged over a user-selected period to reduce scatter. This enables an easier determination of when the heater power and relevant temperatures have settled to steady values, and the final results read from the graphs have high resolution. A researcher measuring thermal conductivity over a limited temperature range could use a routine such as this, but it generally involves a lot of real-time human interaction. We use this program to set up and monitor the pump-out and cool-down, and before the beginning of a data run to determine effective PID parameters for a given sample.

The second routine is a fully-automated data acquisition program for thermal conductivity measurements. It reads pre-determined temperature set-points for the base and the sample and guard floating ends from a configuration file. For each average temperature, four different such balances are established with non-zero temperature drops between the base and the sample floating end. Because of small relative offsets in the calibration of the sample, guard, and base thermometers, it is not possible to consistently control the sample and guard at the same temperature as the base, and including such a "zero ΔT" point actually increases the error in the measurement. While waiting for balance to be achieved, the routine

plots all temperatures and the sample heater power real-time. It also repeatedly stores all values averaged over a period of time selected by the user, usually ten minutes. At the end of each such period, it evaluates the latest data for temperatures and heater power relative to specific criteria to determine if a steady state has been achieved. For the sample heater power and the two intermediate thermometer temperatures, it performs a least-squares fit of each data set to a linear time dependence and compares the slope to the uncertainty in that slope. If a slope is small compared to its own uncertainty, with a pre-chosen comparison factor, the routine treats that data set as steady. For the base and the guard and sample floating ends, their average temperatures over the time period are compared to their individual control set-points. When one of these temperatures matches its set-point to within a pre-selected error, it is considered to be steady. When all five thermometers and the sample heater power are simultaneously steady at the end of a time period, the measurement has achieved balance. For each parameter, the routine stores the average value and standard deviation for the balance time period in a raw data file. After this, it updates the temperature control setpoints to the next set of values in the configuration file to begin the next balance. This process continues until the end of the configuration file is reached.

TEMPERATURE CONTROL

Selecting the best parameters for temperature control in our measurements was originally a challenge. This was particularly true for the sample floating end control, as each sample's thermal conductivity and specific heat are unique. We concluded that the differential control parameter was not helpful and added noise, so we have always used proportional-integral (PI) control. The main difficulty was that the best P and I parameters for maintaining steady temperature control are not well suited for efficiently changing to a new temperature setpoint. We found that the temperature would either "undershoot" or "overshoot" the setpoint, and, for low-conductance samples, the resulting long settling time was very inconvenient.

After years of struggling with this problem, we adopted a simple approach which almost completely eliminated it. Whenever a control channel is moving a temperature to a new setpoint, we initially de-activate the integral control parameter and use "P-only" control. A relatively high proportional gain can be used, and the temperature quickly reaches a stable value slightly below the setpoint. Then we activate the integral control contribution, which brings the temperature to the setpoint without overshooting. Once stable control is achieved, the proportional gain can be lowered to reduce the noise in instantaneous readings. However, with time averaging over ten minute periods, this is generally not necessary. We use the manual-control software to explore the appropriate P and I parameters and the required duration for de-activating the integral. The automated data program is set up to use these values, and we intervene to change them as needed while the average sample temperature steps up from about 4 Kelvin to 295 Kelvin.

DATA ANALYSIS

When the automated program is complete, the raw data file contains four temperature and power data sets for each average temperature between the base and the sample's floating

end, each with a different overall sample temperature drop. This allows us to use a differential version of the thermal conductivity equation, namely

$$\kappa(\bar{T}) = \frac{L}{A}\frac{d\dot{Q}}{d\Delta T}. \tag{3}$$

As mentioned earlier, ΔT is now the difference between the sample's intermediate tap temperatures, $\bar{T}$ is their average value, and L is the distance between the taps. For a given $\bar{T}$, the derivative is determined from a least-squares linear fit of $\dot{Q}$ versus ΔT. Fitting four values allows a reasonable determination of the derivative's uncertainty due to scatter in the data, which would not be possible if only two points were used. This uncertainty is added in root-mean-square fashion to the uncertainties in L and A, resulting in an overall uncertainty in the thermal conductivity at that average temperature.

In general, $\bar{T}$ is not exactly constant for these four balances, unless the intermediate temperature taps are equidistant from the center of the sample. However, it ends up being very close to the constant average of the base and floating end temperatures, so we use this value in equation (3).

The use of a differential measurement technique is very important, as it essentially eliminates the effect of absolute temperature uncertainty due to the calibration curves. For all small values of ΔT about the same average temperature, errors in the indicated tap temperatures remain nearly constant. The result is that there is much less relative uncertainty in $d\dot{Q}/d\Delta T$ than in any single value of $\dot{Q}/\Delta T$. The same is true of the sample floating end and guard temperatures, which are nominally equal. Any relative calibration error in these temperatures is nearly constant for a given $\bar{T}$, so there will be a resulting constant temperature difference between the guard and sample. This will result in a nearly fixed conducted heat between them, but it will not impact the derivative in equation (3).

CALIBRATION CURVE SLOPE UNCERTAINTY

We have explained how our differential measurement drastically reduces errors due to scatter in thermometer calibration curves, but we must discuss how much error remains. First, we consider the impact of the intermediate tap thermometers. To simplify the discussion, we assume that $d\dot{Q}/d\Delta T$ in equation (3) is calculated based on only two different balances. In this case, we are actually measuring $\Delta\dot{Q}/\Delta(\Delta T)$. It is easy to show that the denominator of this ratio is $\Delta T_F - \Delta T_N$, the difference in the changes in the "far" and "near" tap temperatures between the two balances. The uncertainty in each of these denominator terms contributes equally to the denominator's overall uncertainty, and our setpoints are chosen so that $\Delta T_F = -\Delta T_N$. Assuming that the box performs perfect resistance measurements on each thermometer, we can show that

$$\frac{\delta(\Delta(\Delta T))}{\Delta(\Delta T)} = \frac{1}{2}\sqrt{\left(\frac{\delta\left(\frac{dR_F}{dT_F}\right)}{\left(\frac{dR_F}{dT_F}\right)}\right)^2 + \left(\frac{\delta\left(\frac{dR_N}{dT_N}\right)}{\left(\frac{dR_N}{dT_N}\right)}\right)^2}. \tag{4}$$

Thus, it is important to evaluate the relative errors in the dR/dT slopes of the tap thermometer calibration curves, as evaluated by the readout box.

Due to random errors in the calibration process, it is assumed that the calibration points are scattered about a theoretically "true" resistance-versus-temperature curve for each thermometer. LakeShore's estimate of their calibration point uncertainty ranges from +/− 5 mK at 1 K to +/− 40 mK at 300 K. They also provide points computed from a Chebyshev Polynomial fit along with each calibration file, and their website suggests that this "smoothing" fit may be closer to the true curve than are some individual points in the file. For comparison, we also performed a "cubic spline smoothing" fit on the calibration file of an intermediate temperature tap thermometer from our apparatus[7]. These fits use information from a number of calibration points surrounding a given temperature to predict the resistance at that temperature, but neither fit exactly matches any of the original calibration points. The two smoothing fits matched extremely closely, and we assume that the slope of either one is a good estimate of the thermometer's true dR/dT.

In contrast, a cubic spline interpolation of data is forced to exactly match each of the data points. It "zig-zags" above and below the curve generated by a smoothing fit of the same data. Similarly, its slope curve has many crossings of a smoothing fit's slope curve. Since our thermometer readout boxes use a cubic spline interpolation, we evaluated the resulting dR/dT slope differences for the tap thermometer.

Figure 3 compares the slopes of different curves associated with the calibration file of the thermometer mentioned above. The blue dashed curve is the percent slope difference between the cubic spline interpolation of the calibration points and the cubic spline smoothing curve of those points. This gives a good indication of the local error in dR/dT resulting from the controller box's interpolation. Between 6 and 300 K the worst-case error is 0.3%, but over nearly all of this range it is well below 0.2%. Below 6 K the error is higher, but it still less than 1%. This indicates that the potential systematic error due to the interpolation is small compared with the systematic A/L uncertainty for most samples. The red solid curve is the percent slope difference between a cubic spline interpolation of the same calibration's Chebychev fit points and the cubic spline smoothing curve of the original data. Above 5 K this slope difference is well below 0.1%, so the spline interpolation of the Chebychev points has what we assume to be the correct slope. Thus, it would be possible to essentially eliminate possible dR/dT errors by loading the Chebychev calibration points into our controller boxes. We have not historically done this, but we will probably do so for thermal conductivity measurements in the future.

SAMPLE/GUARD MIS-MATCH UNCERTAINTY

We described earlier how the guard and Fiberfrax nearly eliminate radiative heat loss from the sample. For a given average temperature, any thermometer calibration offset between our guard and sample thermometers is likely to remain constant for all four balances. To first order, this will result in a constant heat leak between the guard and sample, which will not affect our power versus ΔT slope. However, the Fiberfrax thermal conductivity is strongly temperature-dependent, so there will be slightly more heat conducted between the sample

and guard for larger ΔT values. This second-order effect will be most important at room temperature, the upper end of our test temperature range. Here the Fiberfrax will have its largest conductivity relative to any realistic sample, and the possible thermometer offset might be as high as 80 mK.

To study the impact of this effect, we made a finite-element thermal model of a hypothetical cylindrical PVC sample inside our 31.75 mm diameter guard. We chose PVC because it has a very low thermal conductivity of 0.16 W/m/K at 300 K, and thus should be susceptible to this error. We modeled four different balances with average temperature of 300 K, each with an 80 mK offset between the sample and guard thermometers. We performed our usual data analysis using the temperatures and power given by the model. The computed thermal conductivity indeed differed visibly from the actual value assumed in modeling the sample.

We repeated this calculation for several different sample diameters between 3 and 30.5 mm. Figure 4 shows a smooth curve fit of these points. For very small sample diameters, the error rises rapidly with decreasing diameter. This is intuitive, since the heat conducted through the sample is proportional to the diameter squared. As the sample diameter approaches that of the guard, heat leaking radially through the Fiberfrax becomes important, and the error rises. Thus, there is an optimum sample diameter, which, for the parameters assumed in this case, occurs around 25 mm. While such a large sample with the necessary thermometers would not fit in our guard, in general it is best to make all sample diameters as large as possible. We expect this error to be inversely proportional to the sample thermal conductivity, so it will be trivially small for nearly all samples we expect to characterize.

TEST RESULTS

We have tested 27 samples in our facility since it was developed in 2004, of which five have been described in previous publications[3,4]. Thirteen samples were customized electrical cables used on JWST. Each cable included numerous metal conductors and shields separated by polymer insulation. While the cross sections of metallic components were well known, the polymer area was always approximate. Thus, we performed a thermal conductance measurement on each type of cable to improve the accuracy of the JWST thermal model. Note that data from these tests were thermal conductances in units of [W·m/K], rather than thermal conductivity values. Since the cables were custom-made for JWST, the results are not of general interest and are not presented here.

Figure 5 shows data for three high-conductivity materials which were candidates for use as a deep-space thermal radiator backing plate. The first of these was aluminum 1350, which is a 99.5% pure aluminum alloy. The second was AlBeMet, a composite product from Materion Corporation made from aluminum and beryllium. The AlBeMet was formed into 1.3 mm thick sheet by a process that involved extrusion and rolling, and we tested samples in the longitudinal and transverse directions relative to that elongation. The longitudinal conduction is measurably higher at low temperatures, but this effect disappears near room temperature. Note that the error bars are smaller than the circle, square and diamond symbols used in the graph.

Figure 6 presents results for two materials of medium thermal conductivity. The Shapal Hi-M Soft, produced by Precision Ceramics, is a machine-able ceramic containing aluminum nitride and boron nitride. The aluminum 6061-T651 was used in a “heat-flow meter,” for which the thermal conductance of a rod needed to fall in a narrow range of values. The solid curve in this figure is the fit provided for aluminum 6061-T6 on the National Institute of Standards and Technology (NIST) materials properties website[8]. This fit is about 30% lower than our data at the lowest temperatures, but it is higher than our data at room temperature. We don’t know the cause of this difference, but it might result from variations in the sample materials. The temper designations T651 and T6 refer to the same heat treatment process, but the former includes a minor plastic stretch of the alloy after the quench[9]. This step is typically included for stress reduction in thick pieces of aluminum, in which there is a significant temperature gradient across the material during the quench. Our sample was cut from a heat-treated 10 cm thick plate, and its properties could be affected by its original depth within the plate. The T6 treatment of the NIST-referenced sample suggests that it was cut from a thinner, more homogeneous piece of alloy. Also, the specification for aluminum 6061 allows for significant variation in the contents of alloying elements. Our sample contained, by weight, 0.7% silicon, 0.46% iron, 0.23% copper, 0.12% manganese, 0.9% magnesium, 0.17% chromium, 0.09% zinc, 0.07% titanium, and 0.04% other elements. In general, we advise anyone needing precise knowledge of an alloy’s thermal conductivity to perform a measurement on a sample cut from the same piece of stock.

Figure 7 shows data for three different polymers. The Epon 815 epoxy sample was cast into a cylindrical shape for our measurement. The other samples were formed by elongation, which tends to align their long molecules and enhance the thermal conductivity in the elongation direction. The Torlon sample was extruded, the Teflon sheet was rolled in one direction, and in both cases we measured the thermal conductivity in the elongated direction. For comparison, the solid line in the graph is a fit to data for what we assume is cast Teflon, from the NIST website[10]. At room temperature the rolled Teflon is nearly three times more conductive than the cast Teflon.

Figure 8 contains data for two different structural composites which are often used in cryogenic space-flight instruments. Both of them provide a good combination of strength, stiffness, and low thermal conductivity. The S2 glass sample had a (45, −45, 0)4s layup in an EX1522 epoxy matrix. The other sample was T300 carbon fiber with a 5HS weave in a (45, 0, −45)2s layup in an RS-3C epoxy matrix. For thermal isolation, T300 is advantageous at lower temperatures, while S-glass is better closer to room temperature.

For the convenience of readers, we performed a curve fit of each data set presented here. The fit form is

$$\kappa(T) = e^{\sum_n A_n [ln(T)]^n}, \quad (5)$$

and the fit coefficients A_n for each material are given in Tables 1 and 2. The number of terms in the summation varies among materials, as indicated by the numbers of coefficients. The units of κ are W/m/K. It should be noted that all of the coefficients’ significant digits given

in the tables must be used, or the resulting fit will not match our data to within the experimental uncertainty.

CONCLUSION

Thermal conductivity measurements between 4 and 300 K with a precision better than 1% are quite feasible, but they require careful attention to detail. In particular, it is important to use a facility and a procedure that are insensitive to first-order errors. Our own facility and staff are generally available to characterize materials over this temperature range for any project with NASA funding.

ACKNOWLEDGEMENTS

The development of our facility and many of the thermal conductivity measurements were supported by NASA's James Webb Space Telescope program.

REFERENCES.

[1]. ASTM Standard E1225–13, "Standard Test Method for Thermal Conductivity of Solids Using the Guarded-Comparative-Longitudinal Heat Flow Technique," ASTM International, West Conshohocken, PA, 2013.

[2]. Moore JP, Williams RK, and Graves RS, Precision measurements of the thermal conductivity, electrical resistivity and Seebeck coefficient from 80 to 400 K and their application to pure molybdenum. Rev. of Sci. Instr, 45(1), 1974, p. 87–95.

[3]. Canavan ER and Tuttle JG, Thermal conductivity and specific heat measurements of candidate structural materials for the JWST optical bench In Advances in Cryogenic Engineering 52, edited by Balachandran U, AIP, 2006, p. 233–240.

[4]. Tuttle JG, Canavan E, and DiPirro M, Thermal and electrical conductivity measurements of CDA 510 phosphor bronze In Advances in Cryogenic Engineering 56, edited by Balachandran U, AIP, 2010, p. 55–62.

[5]. LakeShore Cryotronics Cernox sensor product overview, http://www.lakeshore.com/products/Cryogenic-Temperature-Sensors/Cernox/Models/Pages/Overview.aspx; 2017 [accessed 29.06.17]

[6]. Mukugi K, Tsuchidate H, and Oishi N, Characteristics of cold cathode gauges for outgassing measurements in UHV range. Vacuum, 44, 1993, p. 591–593.

[7]. Powell MJD. Curve fitting by splines in one variable In: Hayes JG, editor. Numerical approximation to functions and data, London: The Athlone Press; 1970, p. 65–83.

[8]. NIST cryogenics technologies group; material properties of 6061-T6 Aluminum, http://cryogenics.nist.gov/MPropsMAY/6061Aluminum/6061_T6Aluminum_rev.htm; 2017 [accessed 29.06.17]

[9]. Chandler H, editor. Heat treater's guide; practices and procedures for nonferrous alloys, Materials Park, Ohio: ASM International; 1996, p.135–145.

[10]. NIST cryogenics technologies group; material properties of Teflon, http://cryogenics.nist.gov/MPropsMAY/Teflon/Teflon_rev.htm; 2017 [accessed 29.06.17]

HIGHLIGHTS

- We developed an apparatus for high-precision thermal conductivity measurements
- Our apparatus and technique avoid many common systematic measurement errors
- We show that the impacts of second-order thermometry effects are insignificant
- We present data graphs for ten different material samples
- We provide curve fits to the data for the convenience of readers

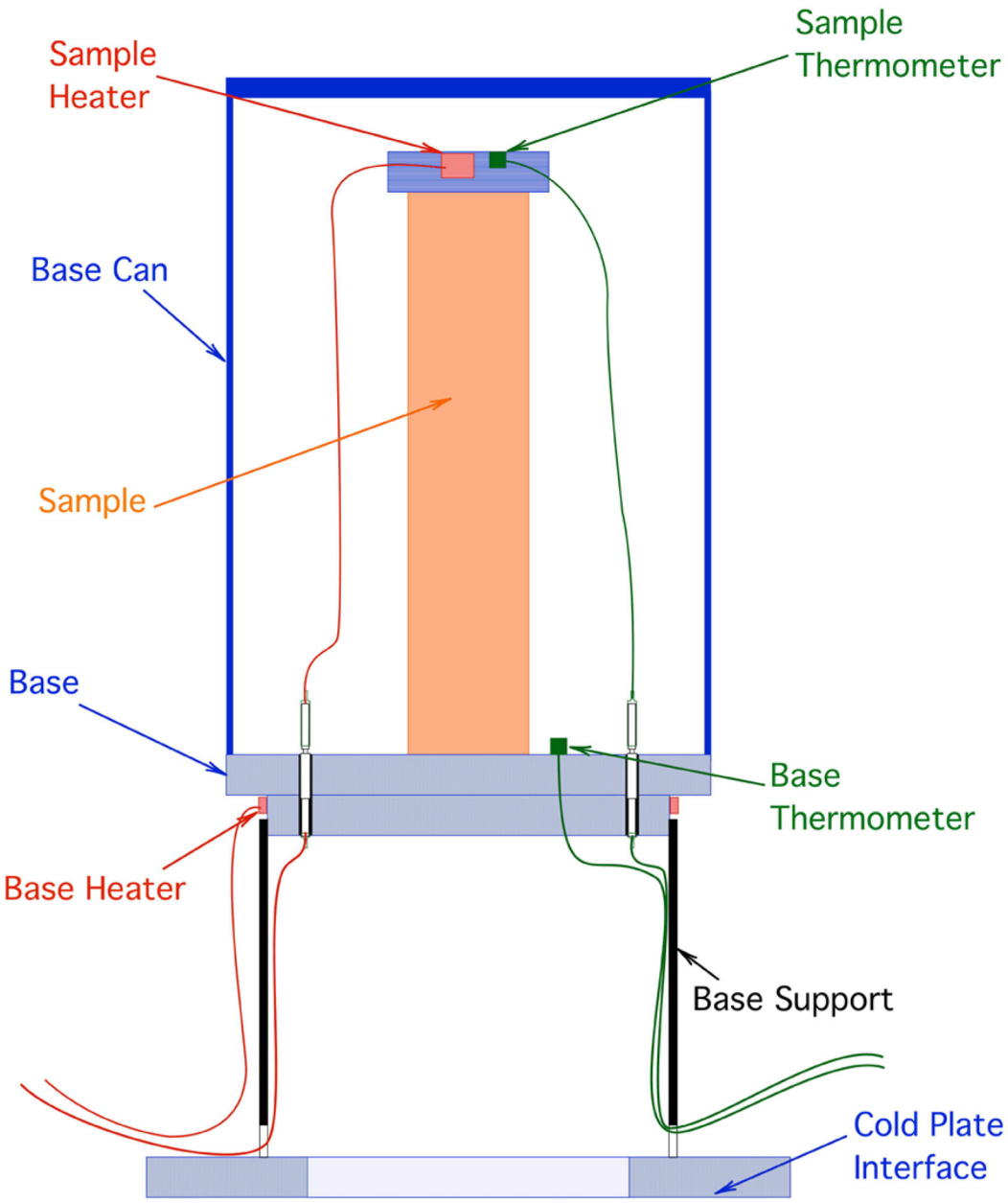

Figure 1.
A schematic representation of a basic thermal conductivity measurement apparatus. There are problems with this approach which make it inappropriate for high-precision measurements.

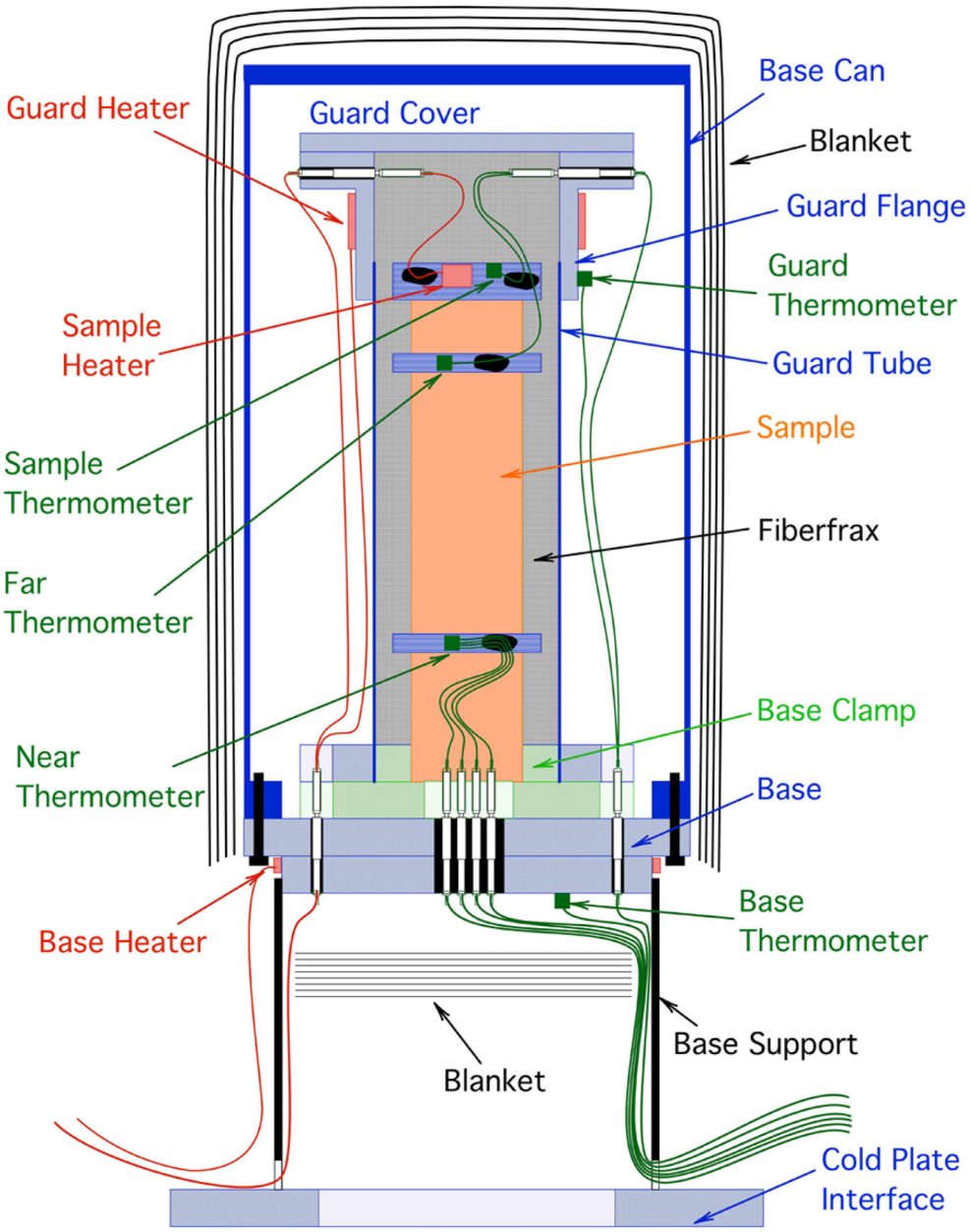

Figure 2.

A schematic view of our enhanced thermal conductivity apparatus, which is appropriate for high-precision measurements between 4 K and room temperature.

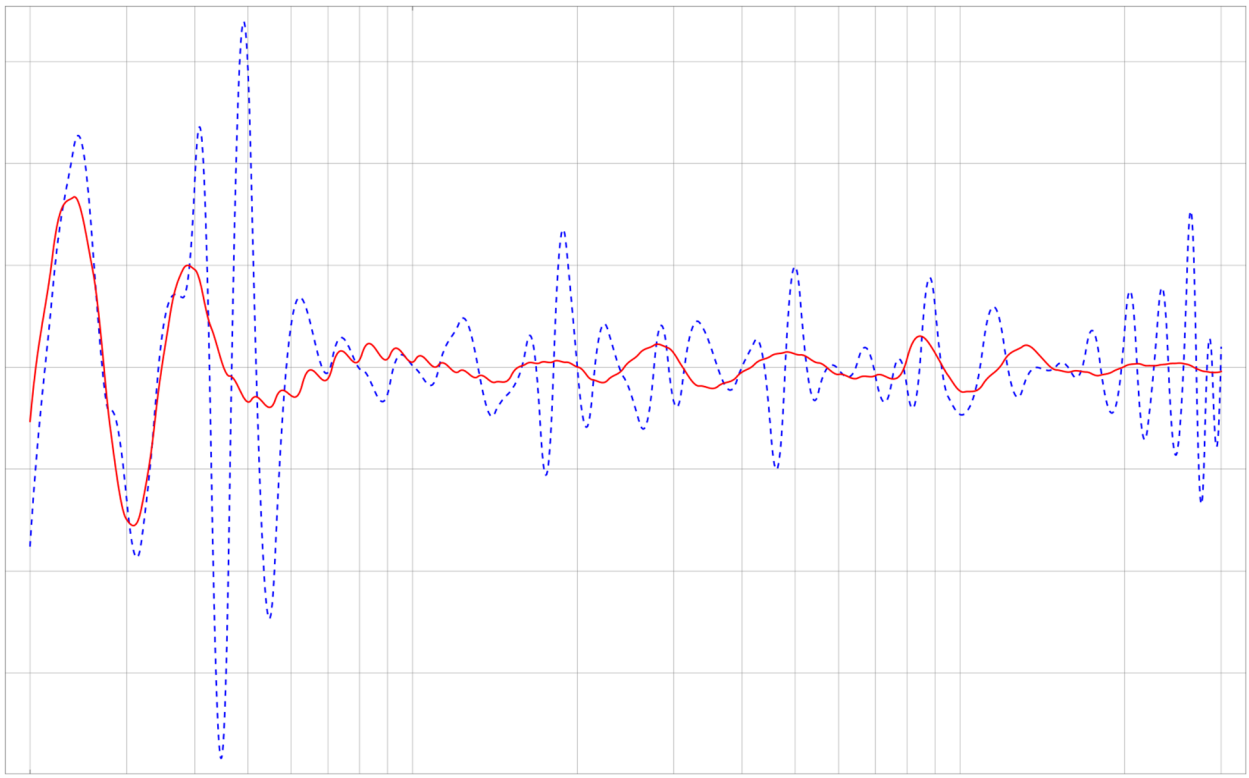

Figure 3.

The slope difference between a spline-smoothed approximation of a thermometer calibration curve, and two different spline interpolations. The blue dashed curve is the difference for an interpolation of raw calibration data. The red solid curve is the difference for an interpolation of points generated using a Chebychev polynomial fit of the calibration points.

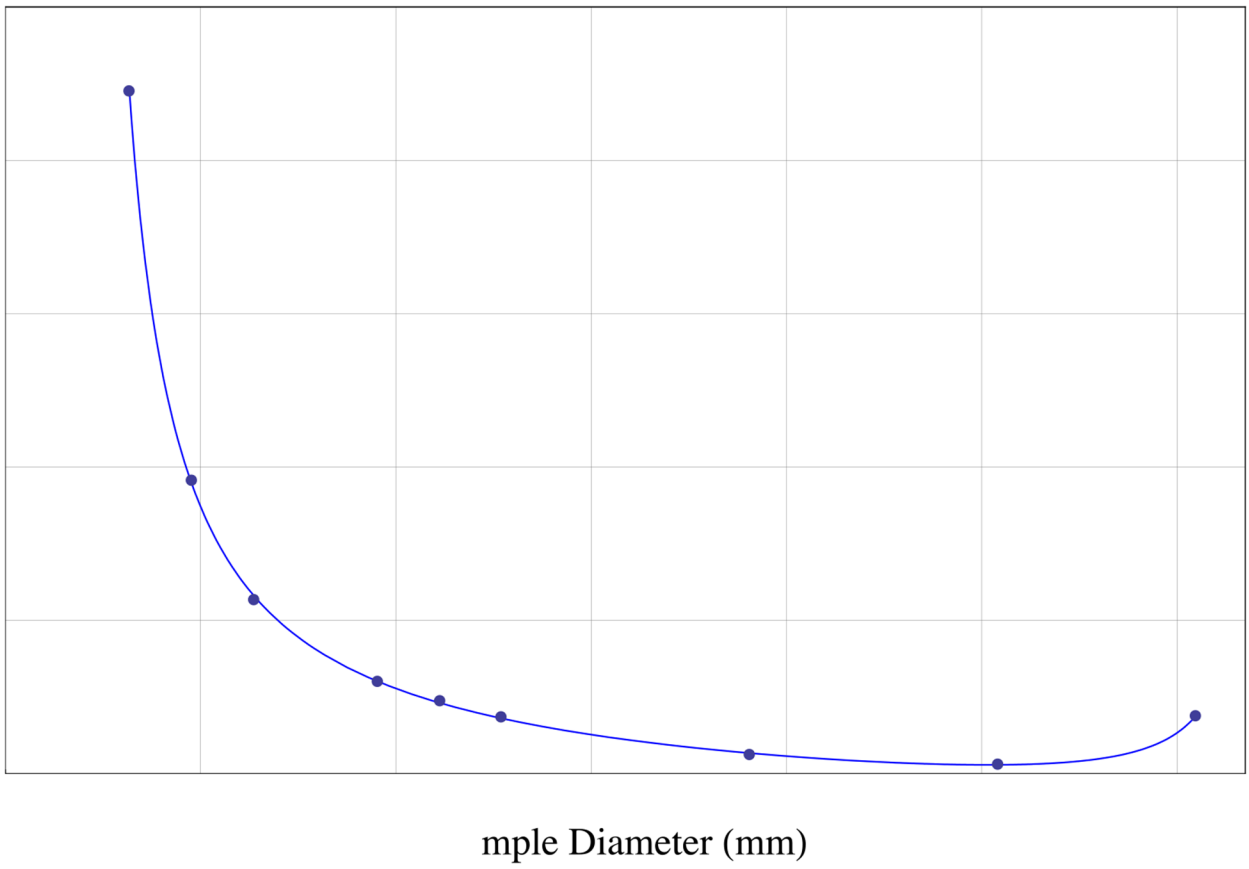

mple Diameter (mm)

Figure 4.

The percent error expected for a 300 Kelvin thermal conductivity measurement of PVC due to a constant 0.08 K mismatch between the sample and base thermometer calibrations.

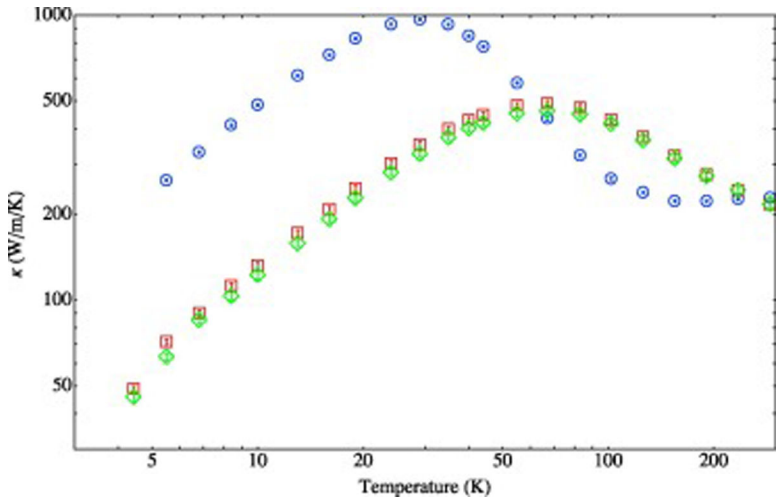

Figure 5.

Thermal conductivity of three different candidates for a radiator substrate. The blue circles are aluminum 1350. The red squares and green diamonds are for AlBeMet sheets oriented in the longitudinal and transverse directions, respectively, relative to their elongation direction during extrusion/rolling.

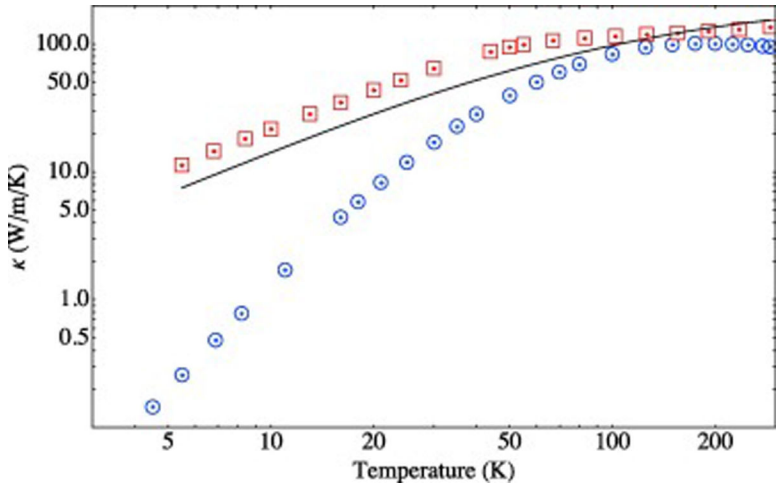

Figure 6.

Data for medium thermal conductivity samples. The red squares are aluminum 6061-T651. The solid curve is the fit provided for aluminum 6061-T6 on the NIST materials properties website. The blue circles are Shapal Hi-M Soft, a machine-able ceramic containing aluminum nitride and boron nitride.

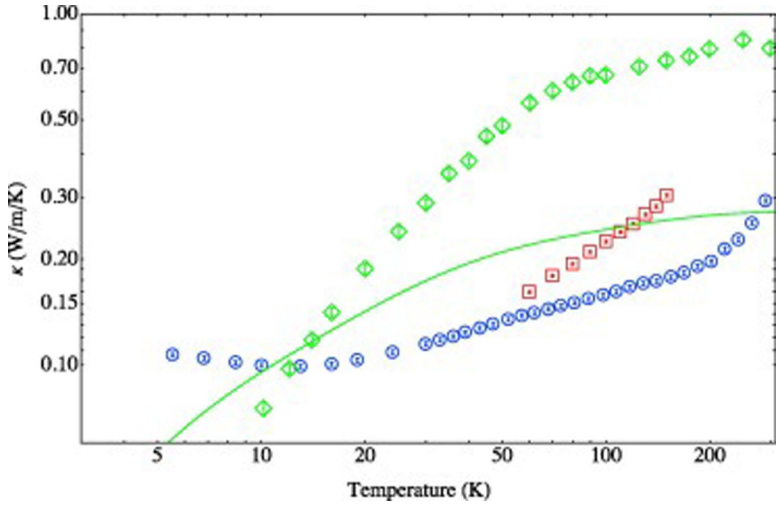

Figure 7.

Thermal conductivity of polymers. The blue circles are Epon 815 epoxy. The red squares are extruded Torlon and green diamonds are rolled Teflon sheet, both measured in the longitudinal direction relative to their elongation. The green solid line is a curve fit for Teflon as listed on the NIST materials properties website.

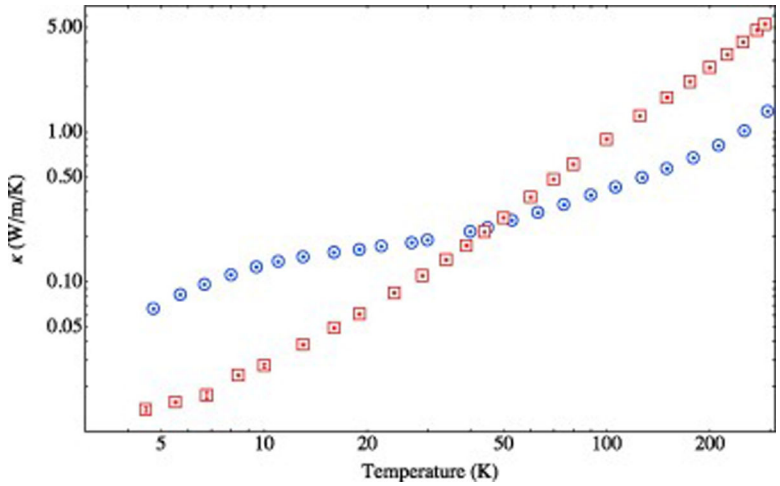

Figure 8.

Thermal conductivity of composites. The blue circles are S-glass [(45, −45,0)4s layup, S2 glass in EX1522 epoxy matrix], and the red squares are T-300 [(45,0, −45)2s layup, T300 carbon fiber with 5HS weave in RS-3C epoxy matrix].

Table 1.

Fit coefficients for several high and medium conductivity samples. The thermal conductivity, κ, in W/m/K, is calculated from: $\kappa(T) = e^{\sum_n A_n [ln(T)]^n}$, with the summation over the number of coefficients listed for each specific sample. Note that the coefficients must contain all of the significant digits shown in the table, or the resulting fit will not match our data to within the experimental uncertainty.

Sample	Aluminum 1350	AlBeMet (Longitudinal)	AlBeMet (Transverse)	Shapal Hi-M Soft	Aluminum 6061
Range (K)	5 to 290	4 to 290	4 to 290	5 to 290	5 to 290
A_0	202.18913	−12.1888	−3.97271	−3.6876776	−15.157786
A_1	−538.40358	29.7292	10.3754	−2.4173503	31.586542
A_2	623.78182	−22.7971	−4.18563	4.2808139	−23.605563
A_3	−400.19331	9.55449	−0.0354217	−1.7313843	9.3260575
A_4	155.65451	−2.28909	0.578585	0.37339127	−1.9804477
A_5	−37.557167	0.317686	−0.181403	−0.043721399	0.21385417
A_6	5.4885214	−0.0245221	0.0224265	0.002113506	−0.009223361
A_7	−0.44454547	0.000845345	−0.00100086		
A_8	0.015306016				

Table 2.

Fit coefficients for thermal conductivity, in W/m/K, of polymer and composite samples. The fit function and the caution regarding significant digits in the coefficients, given in the Table 1 caption, apply here as well.

Sample	Extruded Torlon	Epon 815 Epoxy	Teflon Sheet	S-Glass Composite	T-300 Composite
Range (K)	60 to 150	6 to 290	10 to 299	5 to 295	5 to 290
A_0	−5206.316	0.22522	−107.23044	1.64588	8.3131
A_1	5767.071	−4.8062	170.03226	−14.313	−26.806
A_2	−2554.667	4.1862	−114.46293	15.0661	22.066
A_3	565.4081	−2.0439	40.585704	−7.1898	−9.1176
A_4	−62.51743	0.55823	−7.9233332	1.76388	2.0662
A_5	2.762821	−0.077792	0.80654056	−0.216022	−0.2415
A_6		0.0042945	−0.03348673	0.0105004	0.011366